PHOTONICS Research

Supercontinuum single-photon detector using multilayer superconducting nanowires

Hao Li,[1,2,†] Yong Wang,[1,2,†] Lixing You,[1,2,3,*] Heqing Wang,[1,2] Hui Zhou,[1,3] Peng Hu,[1,2,3] Weijun Zhang,[1,2] Xiaoyu Liu,[1,2] Xiaoyan Yang,[1,2] Lu Zhang,[1,2] Zhen Wang,[1,2] and Xiaoming Xie[1,2]

[1]State Key Laboratory of Functional Materials for Informatics, Shanghai Institute of Microsystem and Information Technology, Chinese Academy of Sciences (CAS), Shanghai 200050, China
[2]CAS Center for Excellence in Superconducting Electronics, Shanghai 200050, China
[3]Center of Materials Science and Optoelectronics Engineering, University of Chinese Academy of Sciences, Beijing 100049, China
*Corresponding author: lxyou@mail.sim.ac.cn

Received 13 August 2019; revised 12 October 2019; accepted 17 October 2019; posted 18 October 2019 (Doc. ID 375337); published 20 November 2019

High-efficiency superconducting nanowire single-photon detectors (SNSPDs), which have numerous applications in quantum information systems, function by using the optical cavity and the ultrasensitive photon response of their ultra-thin superconducting nanowires. However, the wideband response of superconducting nanowires is limited due to the resonance of the traditional optical cavity. Here, we report on a supercontinuum SNSPD that can efficiently detect single photons over an ultra-broad spectral range from visible to mid-infrared light. Our detection approach relies on using multiple cavities with well-separated absorbed resonances formed by fabricating multilayer superconducting nanowires on metallic mirrors with silica acting as spacer layers. Thus, we are able to extend the absorption spectral bandwidth while maintaining considerable efficiency, as opposed to a conventional single-layer SNSPD. Our calculations show that the proposed supercontinuum SNSPD exhibits an extended absorption bandwidth with increased nanowire layers. Its absorption efficiency is greater than 70% over the entire range from 400 to 2500 nm (or 400 to 3000 nm), when using two-layer (or three-layer) nanowires. As a proof of principle, the SNSPD with bilayer nanowires is fabricated based on the proposed detector architecture with simplified geometrical parameters. The detector achieves broadband detection efficiency over 60% from 950 to 1650 nm. This type of detector may replace multiple narrow band detectors in a system and find uses in the emerging and rapidly advancing field of atomic and molecular broadband spectroscopy.

https://doi.org/10.1364/PRJ.7.001425

1. INTRODUCTION

Single-photon detection with quantum-limit sensitivity is a key-enabling technology applied extensively in modern physics, chemistry, biology, and astronomy. Among these, the rapidly advancing quantum information science represented by quantum teleportation and quantum computation in the past decades, has largely motivated the development of single-photon detectors (SPDs). Conventional semiconducting SPDs, such as avalanche photodiodes and photomultiplier tubes, are widely used for visible light detection but suffer from humble performance in detecting near-infrared photons and beyond. In contrast, a superconducting material with an energy gap of several meV, which is almost 1000 times smaller than the bandgap energy of conventional semiconductors, would allow detecting single photons with high efficiency in, but not limited to, the ultraviolet to mid-infrared range [1].

The first superconducting nanowire SPD (SNSPD) demonstrated low detection efficiency due to the limited optical absorption capability of the nanowire [2]. The introduction of optical cavities by fabricating mirror structures in SNSPDs significantly improved their performance [3–7] and led to high detection efficiency close to unity [8–10]. Along with the understanding of the detection mechanism and the improved fabrication and readout techniques, SNSPDs now exhibit considerable advantages over semiconductor SPDs in the performance metrics of detection efficiency, dark count rate, timing jitter, and counting rate, enabling numerous applications such as in lunar–ground laser communication [11], detection loophole-free local realism testing [12], and quantum random number generation [13]. Meanwhile, the applications of SNSPDs were widely extended from ultraviolet to mid-infrared single-photon detection, such as fluorescence detection from trapped ions [14], satellite laser ranging [15,16], singlet oxygen luminescence detection [17], and mid-infrared fluorescence in molecular science [18]. These applications and their associated detectors made full use of the high sensitivity and the

fast and accurate response characteristics of the superconducting nanowire. However, this wideband response is restricted by the resonance of the cavity. Consequently, most SNSPDs work efficiently only over narrow bands around the target wavelengths.

Recently, numerous efforts were made toward developing broadband SNSPDs, whose broadband and high-efficiency features would allow them to be used not only in applications such as photon counting spectrometry, which depend on wideband photon detection, but also in single- or multiple-wavelength applications at ultraviolet to mid-infrared wavelengths. One simple approach to achieve wideband detection is fabricating nanowires atop metallic mirrors with wideband reflectivity and single-layer silica serving as the cavity spacer, in order to expand the absorption spectral bandwidth. Redaelli *et al.* reported a broadband NbTiN-based device with system detection efficiencies (SDEs) greater than 65% in the 1100 to 1550 nm spectral range [19]. Similarly, Wang *et al.* realized a detector with SDEs exceeding 50% in the 950 to 1550 nm spectral range [20]. In addition, multilayer-nanowire structures with separated nanowires provide another method to broaden the bandwidth by increasing the effective optical absorption length without compromising the intrinsic photon response [21–23]. Following this approach, Salim *et al.* theoretically investigated the characteristics of multilayer-nanowire SNSPDs in terms of quantum efficiency and bandwidth. Krapick *et al.* reported an SNSPD with SDE larger than 87% in the spectral range from 1450 to 1640 nm using WSi bilayer nanowires [24] based upon dielectric mirrors. These works are interesting and pave the way for developing SNSPDs with multiple-layer nanowires.

In this work, we report on a supercontinuum SNSPD that can efficiently detect single photons over a spectral range from visible to mid-infrared light. Unlike previously reported broadband SNSPDs [19,20] or SNSPDs with multiple-layer nanowires [21–24], here the multiple cavities with well-separated resonances were introduced into the detector by combining the metallic mirror and well-separated multiple-layer nanowires. This results in a considerably extended absorption spectral bandwidth, while maintaining high efficiency of the SNSPD. Our calculations show a supercontinuum absorption bandwidth with increased layers and absorption efficiency greater than 70% from 400 to 2500 nm (or 400 to 3000 nm) using two-layer (or three-layer) nanowires. Experimentally, the fabricated detector using bilayer nanowires achieves detection efficiencies over 60% from 950 to 1650 nm, verifying its feasibility in practice and its validity in principle. This type of detector may replace multiple narrow band detectors in a system and find uses in the emerging and rapidly advancing field of atomic and molecular broadband spectroscopy.

2. DEVICE DESIGN AND ANALYSIS

A. Materials and Design

Here, we describe the material selection process and the detector structure. First, NbN is selected as the superconducting material because of its relatively high working temperature (approximately 2.1 K) that can be obtained using a compact Gifford-McMahon (G-M) cryocooler. Aluminum is employed as the reflection mirror for its considerable reflectivity over the wavelength range from visible to mid-infrared light. SiO_2 is deployed for the cavity or insulating spacer layer due to its lossless material property in the spectral range under observation. The cross-sectional schematics of the proposed SNSPDs with two- and three-layer nanowires are shown in Figs. 1(a) and 1(c), respectively. The layers of the detector structure, from bottom to top, are Si substrate, metallic mirror, SiO_2 spacer layer, and multiple-layer superconducting nanowires defined by the NbN films and SiO_2 films between with the same linewidth and filling factor. The selected thickness and the width of the superconducting NbN nanowire are 5 and 80 nm, respectively, with a filling factor $f = 0.5$. These dimensions are typical for the SNSPDs to respond to near-infrared photons and beyond. The thicknesses of the substrate and the metal mirror are 400 μm and 100 nm, respectively, and those of the SiO_2 layers, from bottom to top, are referred to as h_1, h_2, and h_3.

The multilayer-nanowire structure has two critical advantages. First, it allows successive and alternative film growth and one final step etching in the fabrication process to ensure the quality of the superconducting films and the fabricated nanowires. Moreover, with the equivalent medium theory in mind [25], the grating-like structure in each layer can be seen as a medium with an equivalent effective material index. Therefore, these multilayer nanowires and the reflecting mirror constitute multiple cavities with varying effective spacer thicknesses, leading to multiple well-separated absorption resonances. SNSPDs with an extended spectral bandwidth can be obtained by tuning the locations of the resonant wavelengths by adjusting the spacer thickness of each layer nanowire (h_1, h_2, and h_3).

In addition to the multilayer nanowires, it is worth noting the importance of the metal-mirror adoption in our detector. As with metallic mirrors, dielectric mirrors were also widely used in high-efficiency SNSPDs [9,24] due to their lossless material property. However, their applications in ultra-broadband SNSPDs are challenging because of their limited reflection bandwidth. Although the reflection bandwidth can easily be extended using serially connected or thickness modulated dielectric mirrors, controlling the reflection phase shift (i.e., the phase dispersion) on the mirror surface remains challenging, which could lead to multiple well-separated absorption bands [26] rather than a supercontinuum absorption spectral bandwidth. In contrast, metallic mirrors exhibit a naturally wide reflection range with ignorable phase dispersion on the mirror surface. Therefore, combining a metallic mirror, instead of a dielectric mirror, with multiple nanowires in supercontinuum detectors is preferable.

B. Analytical Methods and Results

In order to confirm quantitatively the optical properties of the developed multilayer SNSPD, electromagnetic simulation was performed using COMSOL Multiphysics, where the absorption process was modeled as a plane wave interacting with periodic grating [27]. Based on the literature, the refractive indices we used include 3.46 for Si, 1.45 for SiO_2, 0.51–10.72i for Al, and 5.23–5.82i for NbN. Moreover, the material dispersion in the wavelength range under observation was neglected for simplicity. An SNSPD with bilayer nanowires is presented

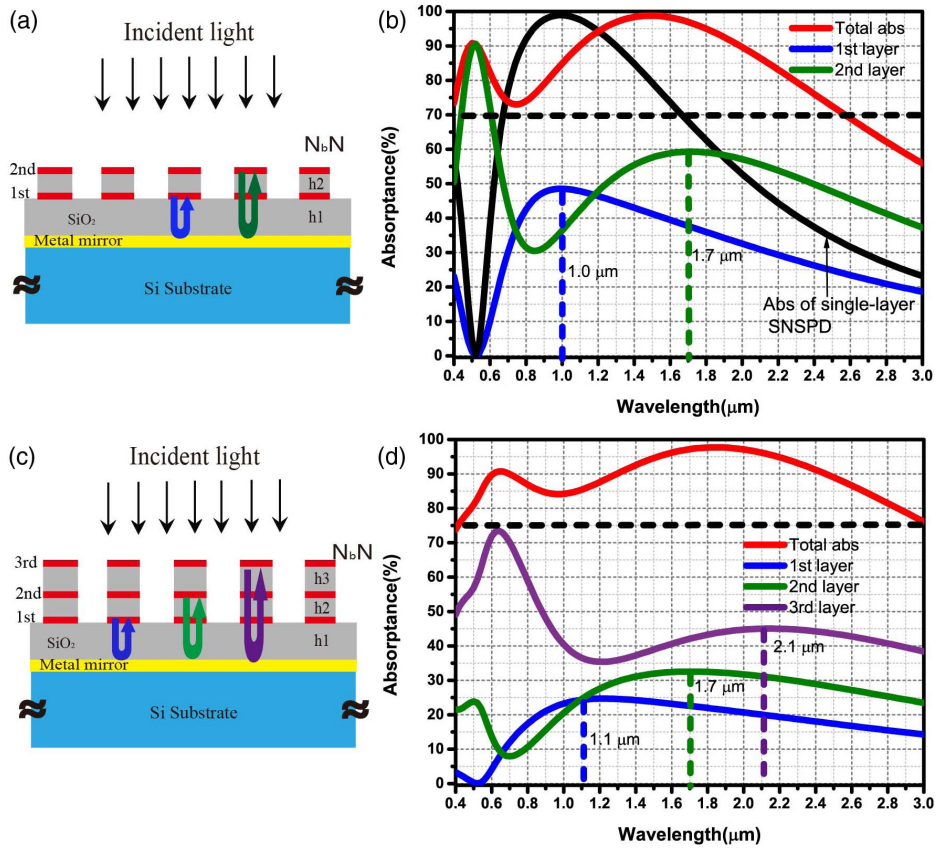

Fig. 1. Cross-sectional schematics of multilayer SNSPDs with (a) two- and (c) three-layer superconducting nanowires. The detector structure includes the following: (bottom to top) Si substrate, Al, SiO_2 layer, and multiple-layer superconducting nanowires. The total absorption (red line) and separated absorption of each layer nanowire of multilayer SNSPDs with (b) two- and (d) three-layer nanowires.

schematically in Fig. 1(a), where the SiO_2 thicknesses are $h_1 = 170$ nm and $h_2 = 70$ nm. Figure 1(b) shows its total absorption (red line) and the absorption of each layer nanowire (blue and green lines). The absorption of the SNSPD using only one nanowire layer with $h_1 = 170$ nm is also indicated with the black line. In comparison, the bilayer SNSPD has an absorption greater than 70% over the spectral range from 400 to 2500 nm, which is much larger than that of the conventional single-layer SNSPD (from 700 to 1600 nm given by the black line). For each layer nanowire of the bilayer SNSPD and the single-layer SNSPD, we observe the resonant maximum and minimum absorption values as functions of the wavelength, which accounts for the limited spectral band of the single-layer nanowire SNSPD. Besides, there is a shift in the absorption curves due to the different effective spacer layer thicknesses, particularly along the peaks at 1.0 and 1.7 μm for the first- and second-layer nanowire, respectively. The combination of these curves with shifted resonances results in the extended spectral range given by the red line in Fig. 1(b).

Further expansion of the absorption spectrum is expected by employing more layer nanowires. In Fig. 1(c), we show an SNSPD with three-layer nanowires and SiO_2 thicknesses $h_1 = 170$ nm, $h_2 = 70$ nm, and $h_3 = 110$ nm. Figure 1(d) shows the calculated absorption of each nanowire layer. The total absorption is greater than 70% from 400 to 3000 nm as indicated with the red line. For each nanowire layer, there is a shift in the absorption curves with increasing effective spacer thickness. Finally, the total absorption curve shows broadband spectral absorption while maintaining considerable efficiency in the entire wavelength range from visible to mid-infrared light.

3. EXPERIMENTS AND RESULTS

Based on the detector architecture proposed above, we fabricate the SNSPD with bilayer nanowires. Note that the cavity spacer layer parameters are set to $h_1 = 190$ nm and $h_2 = 3$ nm. The thin SiO_2 layer (h_2) used here simplifies the fabrication process and the detector readout, while retaining the same underlying physics to broaden the spectral range. In the photon response process, the joule heating generated and the associated phonons upon the photon absorption of one nanowire are transmitted through the thin spacer and trigger the other nanowire [23]. This trigger regime thus enables only a one-channel readout circuit without the after-pulsing issues caused by the electrical instabilities of the conventional avalanched SNSPDs [28,29]. On the other hand, despite the thin spacer layer, the spectrum is expanded due to the slightly separated resonances originating from the two-layer nanowires.

The detector is fabricated on a silicon wafer, where the 100-nm-thick aluminum layer is first deposited on the Si substrate as a reflective mirror, followed by deposition of a 190-nm–thick

SiO_2 layer on the Al mirror. The 6.5-nm–thick NbN layer is deposited on the SiO_2 at room temperature using reactive DC magnetron sputtering in a mixture of Ar and N_2 gases (total pressure: 0.273 Pa). Then, the thin 3-nm SiO_2 is deposited on the NbN film through chemical vapor deposition. The top 6.5-nm-thick layer of NbN is deposited with the same process as the bottom NbN film. The bilayer nanowires covering an active area with a diameter of 15 μm are obtained through electron beam lithography and reactive ions in the CF_4 plasma on the multilayer films. A bridge is finally etched by the reactive ions to form the coplane waveguide for the readout of electrical signals. The final device has a critical temperature of 7.8 K and a switch current of 15.2 μA. Figure 2 presents a scanning electron microscope (SEM) image of the fabricated nanowire with an inset showing the magnified nanowire with the width and pitch of 80 and 160 nm, respectively.

In our measurement, the device is illuminated from the front side using an HI 1060 FLEX single-mode fiber with a core diameter of 6.0 ± 0.5 μm, which is installed in a G-M cryocooler with a working temperature of approximately 2.1 K. The voltage pulse generated by the SNSPD is amplified using a room temperature 50-dB low-noise amplifier (LNA-650, RF Bay Inc.) with a bandwidth of 30 kHz–600 MHz and then input to a pulse counter. In order to measure the detection efficiency, a supercontinuum laser source (NKT: EXB-3) and an acousto-optic tunable filter (NKT: SuperK SELECT) are used to generate a laser beam in the wavelength range of 550 to 1650 nm. The power of the light is attenuated by two attenuators to obtain a number of incident photons of $\sim 10^6$ cps. In addition, a squeeze-type polarization controller (Thorlabs: PLC-900) is used to adjust the light polarization. Here two power meters are used, a power meter (Thorlabs: PM100D) with a photodiode (S150C) to examine the wavelength of 350 to 1100 nm and another power meter (Keysight: 81634B) to calibrate the wavelength of 800 to 1700 nm. The uncertainties of the power meter are 3% and 2.5%, respectively. The laser power fluctuation input to the detector system is approximately 1%, obtained by the power meters. Thus, the measurement errors caused by the calibration of the laser power are 3.2% and 2.7%, respectively [8]. The SDE of the detector is defined as SDE = (PCR – DCR)/PR, where PCR is the output pulse count rate of the SNSPD measured using a pulse counter, DCR is the dark count rate, and PR is the photon rate input to the system. At each bias current, an automated shutter in a variable attenuator blocks the laser light, and the dark counts are collected for 10 s. The light is then unblocked, and the pulse counts are measured by collecting photon counts for another 10 s.

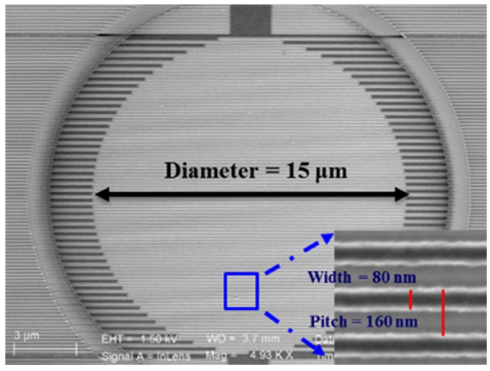

Fig. 2. SEM image of the active area of a bilayer nanowire detector. The inset shows the magnified image of the nanowire. The device diameter, the nanowire width, and the nanowire pitch are 15 μm, 80 nm, and 160 nm, respectively.

Figure 3(a) shows the measured SDEs and DCR as functions of the bias current with wavelengths varying from 1150 to 1650 nm. For these wavelengths, the detector achieves maximum SDEs over 60% and a maximum SDE value of 72.5% at 1250 nm. Note the saturated SDEs and earlier registration at shorter wavelengths, indicating a higher pulse generation probability for large energy photons. The dark hollow square line in Fig. 3(a) shows the variation of DCR with the bias current primarily caused by the black-body radiation of the fiber itself. Figure 3(b) presents the measured SDEs at the bias current of 14.5 μA for wavelengths ranging from 500 to 1700 nm (blue scatters). The detector achieves broadband detection efficiencies with maximum values greater than 60% from 950 to 1650 nm. Although the difference between the experimental result in this study and one of the previous studies [19] is small, we observe a flatter and wider SDE curve over the near-infrared range because of the separated resonances of two cavities, the trend of which coincides well with the theoretical calculation as indicated with the red line.

The timing jitter of the device was measured using a time-correlated single-photon counting module at the wavelength of 1550 nm [30]. Figure 4(a) shows the histogram of the time difference between the laser-synchronizing signal and the device pulse. Here, we define the full width at half-maximum of the histogram as the system timing jitter. Our detector shows a value of 95.0 ps at the bias current $I_b = 14.5$ μA. At the same bias current, the recovery time τ of the device based on the oscilloscope persistence map in Fig. 4(b) is 29.5 ns, which is defined as the duration of the pulse at 1/e of the maximum pulse amplitude.

Finally, to investigate the operational stability of the device, we calculate the autocorrelation function $G(\tau)$ of the photon response, which is the correlation of a signal with a delayed copy of itself as a function of the time delay. For detection pulses generated from a continuous-wave laser, $G(\tau)$ reflects the characteristics of the detector itself. As shown in Fig. 5, a flat $G(\tau)$ with a value of 1.0 is obtained at a bias current of 14.5 μA, indicating the absence of after-pulses during the operation of the detector. This means that no electrical avalanche participates in the detection event [29]. In addition, the fact that $G(\tau)$ increases rapidly to 1.0 in the temporal range in the autocorrelation curve reflects the detector's dead time. Here, we define the dead time as the time needed for $G(\tau)$ to increase to 0.9 (60 ns at 14.5 μA). This value is greater than the one acquired from Fig. 4(b), which indicates that the value based on the oscilloscope persistence trace is merely an ideal condition.

4. DISCUSSION

In principle, the SDE of SNSPD is primarily determined by the intrinsic photon response probability of the superconducting

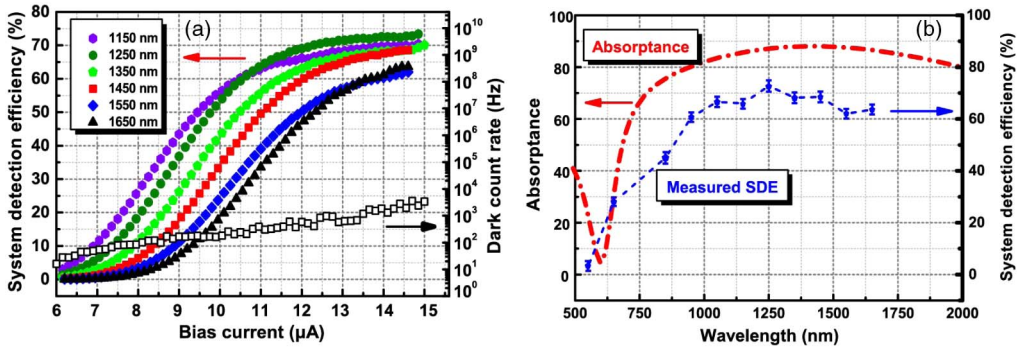

Fig. 3. (a) SDE versus bias current at different wavelengths (the dark square line is DCR as a function of bias current). (b) SDE as a function of wavelength from 500 to 1700 nm (blue line), and the red line is the simulated absorptance for comparison.

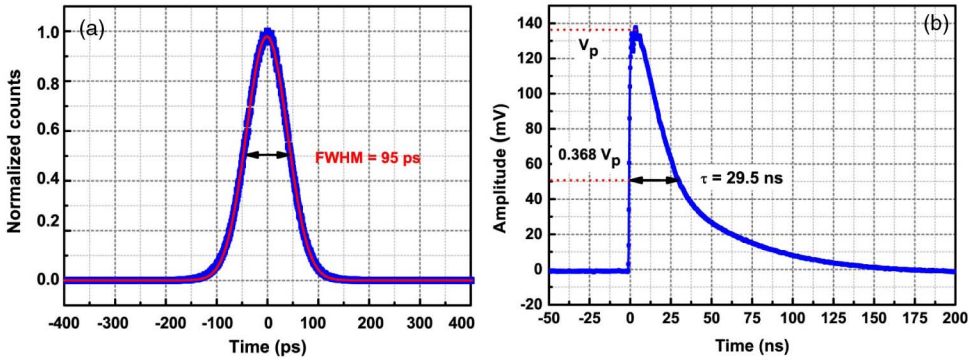

Fig. 4. (a) Histogram of time-correlated photon counts measured at a wavelength of 1550 nm (blue circle; the red line is the fitted curve using Gaussian distribution). (b) Oscilloscope persistence map of the response at a bias current of 14.5 μA.

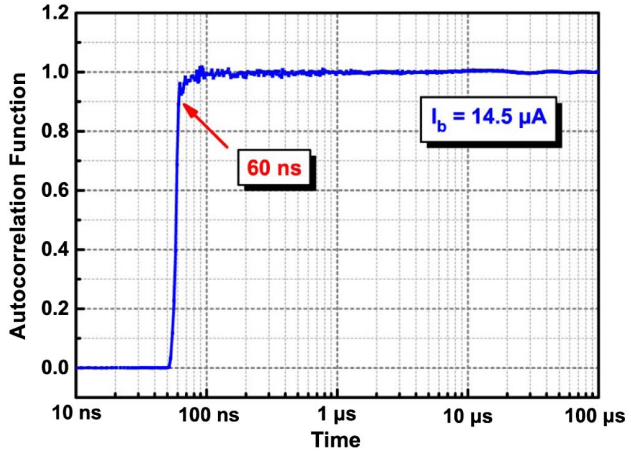

Fig. 5. Autocorrelation function $G(\tau)$ at the bias current of 14.5 μA.

nanowire and the absorption efficiency of the detector, in addition to the optical path loss in the detection system. Recent reports have shown that the intrinsic efficiency becomes close to unity toward mid-infrared photons by decreasing the geometrical size of the nanowire [1], or adopting a superconducting material with a lower-energy gap such as WSi [31]. The multilayer optical structure combined with the ultra-broadband response capability of the superconducting nanowire promises a supercontinuum SNSPD with considerable detection efficiency over the entire spectral range from visible to near-infrared photons and beyond.

Experimentally, we fabricate a bilayer SNSPD, which achieves broadband detection with efficiencies greater than 60% from 950 to 1650 nm. The difference between the experimental result and the calculation may be attributed to the optical loss caused by the imperfect fabrication of the device or the optical coupling loss between the fiber and the nanowire region. The fabrication and the optical coupling optimization are thus required to increase the detection efficiency. On the other hand, here the experimental result is a proof-of-principle demonstration toward a supercontinuum SNSPD using a multilayer-nanowire structure. Detailed improvement and optimizations for both the superconducting nanowire and the optical structure parameters are required in order to expand the bandwidth further. Regarding the intrinsic photon response, the fabricated nanowires have a thickness of 6.5 nm, line-width of 80 nm, critical temperature of 7.8 K, and switch current of 15.2 μA. These nanowire parameters correspond to a nearly saturated response of at most 1650 nm photons, as shown in Fig. 3(a). Thus, decreasing the size of the nanowires (thickness and line-width), using optimized or postprocessed

superconducting materials or other superconducting materials with a lower-energy gap such as WSi, is necessary. Moreover, the cavity spacer layer used here results in absorption resonances of bilayer nanowires that are slightly separated by several nanometers. In order to expand the bandwidth to the visible light range, we should decrease the large spacer layer h_1 and increase the small spacer layer h_2, as given in Fig. 1(b). Compared to the single-layer SNSPD, attention should also be paid to the photoresist selection and the etching process for multilayer superconducting nanowire structure regarding the device fabrication.

Finally, we emphasize the detector development and its potential applications. To date, SNSPD performance has been largely improved in terms of detection efficiency, timing resolution, and detection speed. Meanwhile, readout techniques are also well developed for detector arrays that are capable of resolving the spatial coordinates. The multilayer supercontinuum SNSPD reported here can be applied to detect wide wavelength range photons for various spectroscopy applications. We may envision the combination of these techniques for multidimensional single-photon detection that can detect efficiently and accurately the photon distribution versus wavelength, time, and spatial coordinates.

5. CONCLUSIONS

In conclusion, we report on multilayer-nanowire SNSPDs that can detect ultra-broad photons by leveraging multiple cavities. Our calculation shows absorption efficiencies greater than 70% over the entire range from 400 to 2500 nm (or 400 to 3000 nm) when using two-layer (or three-layer) nanowires. We fabricate a bilayer SNSPD that achieves broadband detection with efficiencies greater than 60% from 950 to 1650 nm. This SNSPD type may replace multiple narrow band detectors in a system and be applied in the emerging and rapidly advancing field of atomic and molecular broadband spectroscopy.

Funding. National Key Research and Development Program of China (2017YFA0304000); National Natural Science Foundation of China (61671438, 61827823, 61971408); Science and Technology Commission of Shanghai Municipality (16JC1400402, 18511110200, 18XD1404600).

†These authors contributed equally to this work.

REFERENCES

1. F. Marsili, F. Bellei, F. Najafi, A. E. Dane, E. A. Dauler, R. J. Molnar, and K. K. Berggren, "Efficient single photon detection from 500 nm to 5 μm wavelength," Nano Lett. **12**, 4799–4804 (2012).
2. G. N. Gol'tsman, O. Okunev, G. Chulkova, A. Lipatov, A. Semenov, K. Smirnov, B. Voronov, A. Dzardanov, C. Williams, and R. Sobolewski, "Picosecond superconducting single-photon optical detector," Appl. Phys. Lett. **79**, 705–707 (2001).
3. K. M. Rosfjord, J. K. W. Yang, E. A. Dauler, A. J. Kerman, V. Anant, B. M. Voronov, G. N. Gol'tsman, and K. K. Berggren, "Nanowire single-photon detector with an integrated optical cavity and anti-reflection coating," Opt. Express **14**, 527–534 (2006).
4. T. Yamashita, S. Miki, H. Terai, and Z. Wang, "Low-filling-factor superconducting single photon detector with high system detection efficiency," Opt. Express **21**, 27177–27184 (2013).
5. S. Miki, T. Yamashita, H. Terai, and Z. Wang, "High performance fiber-coupled NbTiN superconducting nanowire single photon detectors with Gifford-McMahon cryocooler," Opt. Express **21**, 10208–10214 (2013).
6. V. B. Verma, B. Korzh, F. Bussières, R. D. Horansky, S. D. Dyer, A. E. Lita, I. Vayshenker, F. Marsili, M. D. Shaw, H. Zbinden, R. P. Mirin, and S. W. Nam, "High-efficiency superconducting nanowire single-photon detectors fabricated from MoSi thin-films," Opt. Express **23**, 33792–33801 (2015).
7. D. Rosenberg, A. J. Kerman, R. J. Molnar, and E. A. Dauler, "High-speed and high-efficiency superconducting nanowire single photon detector array," Opt. Express **21**, 1440–1447 (2013).
8. F. Marsili, V. B. Verma, J. A. Stern, S. Harrington, A. E. Lita, T. Gerrits, I. Vayshenker, B. Baek, M. D. Shaw, R. P. Mirin, and S. W. Nam, "Detecting single infrared photons with 93% system efficiency," Nat. Photonics **7**, 210–214 (2013).
9. W. Zhang, L. You, H. Li, J. Huang, C. Lv, L. Zhang, X. Liu, J. Wu, Z. Wang, and X. Xie, "NbN superconducting nanowire single photon detector with efficiency over 90% at 1550 nm wavelength operational at compact cryocooler temperature," Sci. China Phys. Mech. **60**, 120314 (2017).
10. H. Le Jeannic, V. B. Verma, A. Cavailles, F. Marsili, M. D. Shaw, K. Huang, O. Morin, S. W. Nam, and J. Laurat, "High-efficiency WSi superconducting nanowire single-photon detectors for quantum state engineering in the near infrared," Opt. Lett. **41**, 5341–5344 (2016).
11. H. Hemmati, D. M. Boroson, D. M. Boroson, B. S. Robinson, D. V. Murphy, D. A. Burianek, F. Khatri, J. M. Kovalik, Z. Sodnik, and D. M. Cornwell, "Overview and results of the Lunar Laser Communication Demonstration," Proc. SPIE **8971**, 89710S (2014).
12. M. Li, C. Wu, Y. Zhang, W. Liu, B. Bai, Y. Liu, W. Zhang, Q. Zhao, H. Li, Z. Wang, L. You, W. J. Munro, J. Yin, J. Zhang, C. Peng, X. Ma, Q. Zhang, J. Fan, and J. Pan, "Test of local realism into the past without detection and locality loopholes," Phys. Rev. Lett. **121**, 080404 (2018).
13. Y. Liu, Q. Zhao, M. Li, J. Guan, Y. Zhang, B. Bai, W. Zhang, W. Liu, C. Wu, X. Yuan, H. Li, W. J. Munro, Z. Wang, L. You, J. Zhang, X. Ma, J. Fan, Q. Zhang, and J. Pan, "Device-independent quantum random-number generation," Nature **562**, 548–551 (2018).
14. D. H. Slichter, V. B. Verma, D. Leibfried, R. P. Mirin, S. W. Nam, and D. J. Wineland, "UV-sensitive superconducting nanowire single photon detectors for integration in an ion trap," Opt. Express **25**, 8705–8720 (2017).
15. H. Li, S. Chen, L. You, W. Meng, Z. Wu, Z. Zhang, K. Tang, L. Zhang, W. Zhang, X. Yang, X. Liu, Z. Wang, and X. Xie, "Superconducting nanowire single photon detector at 532 nm and demonstration in satellite laser ranging," Opt. Express **24**, 3535–3542 (2016).
16. L. Xue, Z. Li, L. Zhang, D. Zhai, Y. Li, S. Zhang, M. Li, L. Kang, J. Chen, P. Wu, and Y. Xiong, "Satellite laser ranging using superconducting nanowire single-photon detectors at 1064 nm wavelength," Opt. Lett. **41**, 3848–3851 (2016).
17. N. R. Gemmell, A. McCarthy, B. Liu, M. G. Tanner, S. D. Dorenbos, V. Zwiller, M. S. Patterson, G. S. Buller, B. C. Wilson, and R. H. Hadfield, "Singlet oxygen luminescence detection with a fiber-coupled superconducting nanowire single-photon detector," Opt. Express **21**, 5005–5013 (2014).
18. L. Chen, J. A. Lau, D. Schwarzer, J. Meyer, V. B. Verma, and A. M. Wodtke, "The Sommerfeld ground-wave limit for a molecule adsorbed at a surface," Science **363**, 158–161 (2019).
19. L. Redaelli, G. Bulgarini, S. Dobrovolskiy, S. N. Dorenbos, V. Zwiller, E. Monroy, and J. M. Gérard, "Design of broadband high-efficiency superconducting-nanowire single photon detectors," Supercond. Sci. Tech. **29**, 065016 (2016).
20. Y. Wang, H. Li, L. You, C. Lv, J. Huang, W. Zhang, L. Zhang, X. Liu, Z. Wang, and X. Xie, "Broadband near-infrared superconducting nanowire single-photon detector with efficiency over 50%," IEEE Trans. Appl. Supercond. **27**, 2200904 (2017).
21. I. N. Florya, Y. P. Korneeva, M. Y. Mikhailov, A. Y. Devizenko, A. A. Korneev, and G. N. Goltsman, "Photon counting statistics of superconducting single-photon detectors made of a three-layer WSi film," Low Temp. Phys. **44**, 221–225 (2018).

22. A. J. Salim, A. Eftekharian, and A. H. Majedi, "High quantum efficiency and low dark count rate in multi-layer superconducting nanowire single-photon detectors," J. Appl. Phys. **115**, 054514 (2014).
23. V. B. Verma, A. E. Lita, M. J. Stevens, R. P. Mirin, and S. W. Nam, "Athermal avalanche in bilayer superconducting nanowire single-photon detectors," Appl. Phys. Lett. **108**, 131108 (2016).
24. M. H. S. Krapick, V. B. Verma, I. Vayshenker, S. W. Nam, and R. P. Mirin, "Superconducting single-photon detectors with enhanced high-efficiency bandwidth," arXiv:1706.00004 (2017).
25. B. Sareni, L. Krähenbühl, A. Beroual, and C. Brosseau, "Effective dielectric constant of periodic composite materials," J. Appl. Phys. **80**, 1688–1696 (1996).
26. H. Li, H. Wang, L. You, P. Hu, W. Shen, W. Zhang, X. Yang, L. Zhang, H. Zhou, Z. Wang, and X. Xie, "Multispectral superconducting nanowire single photon detector," Opt. Express **27**, 4727–4733 (2019).
27. V. Anant, A. J. Kerman, E. A. Dauler, J. K. W. Yang, K. M. Rosfjord, and K. K. Berggren, "Optical properties of superconducting nanowire single-photon detectors," Opt. Express **16**, 10750–10761 (2008).
28. F. Marsili, F. Najafi, E. Dauler, R. J. Molnar, and K. K. Berggren, "Afterpulsing and instability in superconducting nanowire avalanche photodetectors," Appl. Phys. Lett. **100**, 112601 (2012).
29. S. Miki, M. Yabuno, T. Yamashita, and H. Terai, "Stable, high-performance operation of a fiber-coupled superconducting nanowire avalanche photon detector," Opt. Express **25**, 6796–6804 (2017).
30. L. You, X. Yang, Y. He, W. Zhang, D. Liu, W. Zhang, L. Zhang, L. Zhang, X. Liu, S. Chen, Z. Wang, and X. Xie, "Jitter analysis of a superconducting nanowire single photon detector," AIP Adv. **3**, 072135 (2013).
31. L. Chen, D. Schwarzer, J. A. Lau, V. B. Verma, M. J. Stevens, F. Marsili, R. P. Mirin, S. W. Nam, and A. M. Wodtke, "Ultra-sensitive mid-infrared emission spectrometer with sub-ns temporal resolution," Opt. Express **26**, 14859–14868 (2018).